JPE 5-1-6

Performances of SRM for LSEV

Jin-Woo Ahn†, Tae-Hyoung Kim* and Dong-Hee Lee**

†*Dept. of Electrical and Mechatronics Eng., Kyungsung Univ., Korea
**OTIS-LG, Korea

ABSTRACT

This paper presents an application of SR drives for LSEV's(Low Speed Electric Vehicles) which are used for golf and leisure. Two types of 5[HP] SRM's and its drive system are designed and tested. In order to be energy saving and have effective braking during deceleration, a multi-level inverter is proposed. For the precise switching angle control, a new type of analog encoder is proposed. A current control is adopted for soft starting and an angle control is adopted at high speed to increase efficiency. Drive characteristics and performance are shown with test results.

Keywords: Switched Reluctance Motor, Traction drive, Multi-level inverter, Analog encoder, Angle control, Current control

1. Introduction

Nowadays, exhaust control is more consolidating all over the world because of serious air and environmental pollution. Strenuous efforts have been made to reduce pollution. For these reasons, some motor companies have developed HEV's(hybrid electric vehicles) which have a mechanical engine and motor drive with a battery. An EV which uses only a battery and motor drive is also being widely developed. Actually, the pure EV has higher energy efficiency than an engine or a HEV. It also has the advantage of reducing air pollution. Although the EV system battery is expensive and lack of charging infra, various EVs are being developed for leisure and medical care.

Manuscript received August 5, 2004; revised Nov. 17, 2004.
† Corresponding Author: jwahn@ks.ac.kr, Kyungsung Univ.
Tel: +82-51-620-4770, Fax: +82-51-624-5980
* Dept. of Electrical and Electronics Eng., Graduate school, Kyungsung Univ.
** OTIS-LG.

Because of reliability and mechanical strength, brushless type motors such as induction and permanent AC motors are frequently considered for EV traction. Recently SRM's(switched reluctance motors) has been investigated for EV applications due to their mechanical strength and cost advantages[1]. The SRM is a simple, low-cost, and robust motor suitable for variable-speed and traction applications[2]. In addition, the SRM has a high power-to-weight and torque-to-weight ratio, a wide speed range and excellent starting characteristics. Therefore, it is suitable for traction drives which are frequently stopped and started such as those used in electric cars.

In this paper, the SRM drive system is studied for LSEV use for leisure and golf. First, the motor is designed to meet the restricted space requirements. Next, from a CAD and a FEM analysis of efficiency and output characteristics based on the rotor and stator structure, detailed design parameters are determined.

In order to have effective energy regeneration during deceleration and braking, a novel multi-level inverter is

introduced. The proposed multi-level inverter is suitable for exciting and demagnetizing a phase rapidly. A single-pulse exciting method is also introduced to prevent the decrease of efficiency and torque under light load conditions.

In addition, a new low-cost analog encoder is presented to provide precise switching angle control suitable for this drive. In this encoder the switch on-off angle is controlled with a simple circuit. The proposed switching technique is different from the general methods as the resolution of the switch on-off angle is not affected by the sampling period of the microprocessor or the speed of the motor. Hence, the on-off switching angle control can be always carried out at any desired positions.

2. Configurations of LSEV and Specifications

Fig. 1 shows the configuration of the LSEV discussed in this paper. This configuration is simpler than the HEV because an engine control system is not required. The main power source is a battery which is controlled by a BMS(battery management system) and a battery charger. Additionally, regenerative energy is returned to the battery during braking and deceleration.

It has rear drive system which has a 10:1 gear box ratio to transfer the driving power from the motor to the wheel shaft. The maximum speed is 40[km/h] in street mode and 20[km/h] in golf mode.

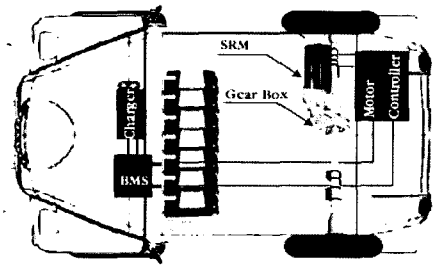

Fig. 1 Configuration of LSEV system

The required maximum speed of the motor can be easily obtained from the maximum speed as follows.

$$\omega_{rm\_max} = \frac{LSEV\ Speed \cdot \eta \cdot 1000}{2\pi \cdot D \cdot 60} \quad (1)$$

where, LSEV Speed : required maximum speed [km/h], η : gear ratio, D : diameter of wheel[m]

In this application, the motor speed required to satisfy the drive speed is about 3600[rpm]. Table 1 shows the specifications of the motor for the LSEV.

Table 1 The specification of SRM for LSEV

Output power	3.5[kw] continuous, 9[kw] 2minutes
Voltage	72[V] (50 ~ 90[V])
Torque	10[Nm] at 4000rpm, 22[Nm] at 2000rpm
Weight	16[kg] below
Size	180[mm] × 190[mm] below
Insulation	H grade
Cooling	Air cooling
Efficiency	80% over

The size and weight of the motor drive system are restricted by vehicle space. The supply voltage is determined by the battery.

3. Design of Motor for LSEV

3.1 Basic principle

The SRM is a doubly salient, singly excited machine and the developed torque is produced by the reluctance variations. The torque is proportional to the square of the switching mmf current and the gradient of phase inductance according to the rotor angular position as shown in (2).

$$T(\theta,i) = \frac{\partial W(\theta,i)}{\partial \theta} = \frac{1}{2}\frac{\partial L(\theta,i)}{\partial \theta} i^2 \quad (2)$$

where i denotes the phase current and L(θ) is the nonlinear inductance profile as a function of the angular rotor position.

The instantaneous voltage equation depends on the nonlinear winding impedance and the phase current as follows.

$$V(\theta) = R \cdot i(\theta) + L(\theta)\frac{di(\theta)}{d\theta} + i(\theta)\frac{dL(\theta)}{d\theta} \qquad (3)$$

Where the first term on the right is the resistance voltage drop, the second is the reactance voltage drop, and the last is the back speed e.m.f which can be converted to mechanical energy. In the instantaneous voltage equation, the phase current for torque production depends on the winding impedance, the speed e.m.f., the switching-on/off angle and the applied voltage. The first and second factors depend on the motor and operating speed. The third and last factors can be adjusted by the controller with a proper control algorithm. Therefore, the design parameters of the motor are determined by the restricted supplied voltage and the rated speed in the actual application. The advance angle and applied voltage can be controlled to assure a stable and highly efficient drive.

3.2 Comparisons of Design Results

Although there are some advantages to SRM's, their actual application is very restricted because of acoustic noise and mechanical vibration. The design specifications have some requirements such as torque and speed, and restricted terms such as supply voltage and dimensions.

The design process of SRM's is different from that of conventional DC and AC motors because SRM uses reluctance torque whose characteristics vary greatly according to the selection of stator and rotor poles.

The general combinations of stator and rotor pole arrays are 6/4, 8/6, 12/8 and 16/12. However, 8/6 and 16/12 SRM's are not preferred for LSEV applications because of the complexity and cost of the four-phase inverter. In this paper, the characteristics of 6/4 and 12/8 SRM's are compared and tested.

Fig. 2 and 3 show the FEM analysis and comparison of 6/4 and 12/8 SRM's according to stator and rotor pole arc, stroke angle(ε_0), and yoke ratio. The analysis results show that the torque and efficiency of a 6/4 SRM is higher than that of a 12/8 SRM.

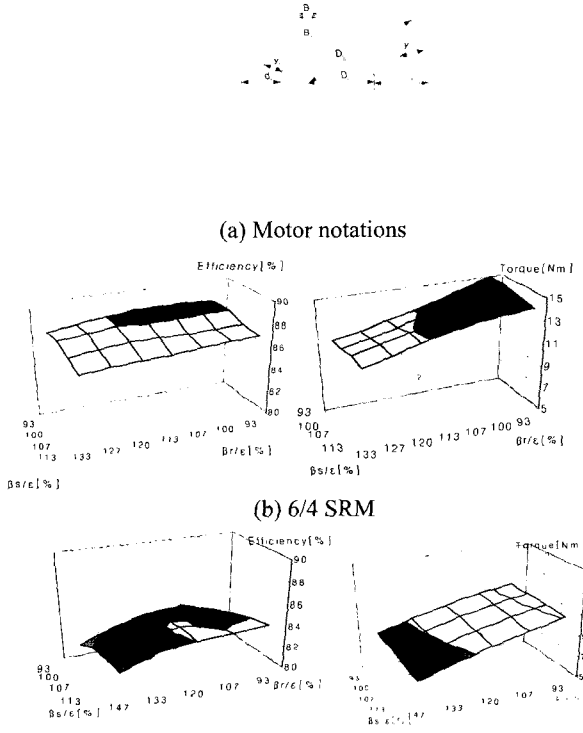

(a) Motor notations

(b) 6/4 SRM

(c)12/8 SRM

Fig. 2 Performance comparisons of FEM analysis according to rotor and stator pole arc

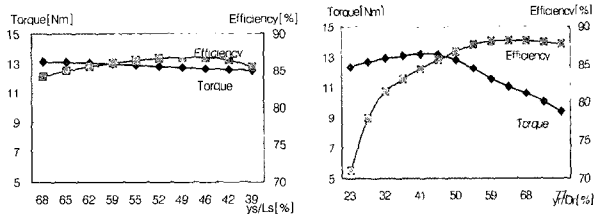

(a) Torque and efficiency of 6/4 SRM

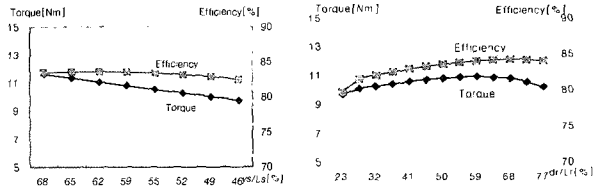

(b)Torque and efficiency of 12/8 SRM

Fig. 3 Performance analysis according to rotor and stator yoke

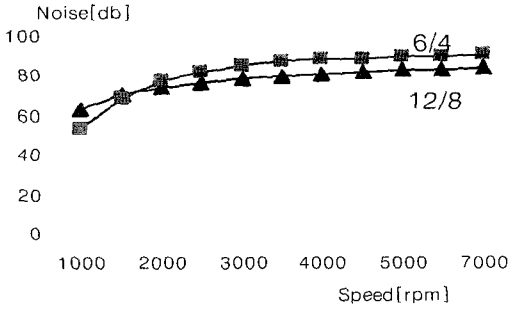

Fig. 4 Simulation result of acoustic noise

Fig. 4 shows the simulation result for acoustic noise of 6/4 and 12/8 SRM's. The acoustic noise of a 12/8 SRM is lower than that of a 6/4 SRM because the torque ripple and rebounding force of a 6/4 SRM is higher than that of a 12/8 SRM at the instant the motor is switched off.

From the analysis, the final dimensions are determined which satisfy the application requirements. Table 2 and Fig. 5 show the detailed design parameters calculated from the analysis of characteristics according to the parameter variations.

Table 2 Design parameters of the prototype SRM

Motor	6/4	12/8
Ns	6	12
Nr	4	8
Stator pole arc [deg]	34	14
Rotor pole arc[deg.]	36	16
Dia. Stator[mm]	138	138
Dia. Rotor[mm]	76	76
Stator yoke[mm]	14	16
Rotor yoke[mm]	9	11
Airgap[mm]	0.25	0.25
Stack length[mm]	100	100
Turn per phase[mm]	11	20
Dia. Conductor[mm]	1.9	1.7

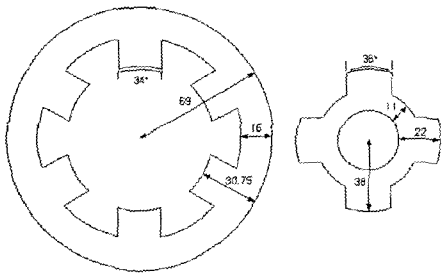

(a) 6/4 SRM

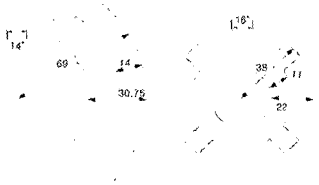

(b) 12/8 SRM

Fig. 5 Cross sectional dimensions of prototype SRM

12/8 SRM's operate with less torque ripple and acoustic noise, but 6/4 SRM's provide better torque and efficiency.

Fig. 6 shows the photograph of the prototype 6/4 and 12/8 SRM's. In order to verify the effectiveness of the proposed SRM system in the LSEV application, the prototype 6/4 and 12/8 SRM's with analog encoders and multi-level inverters are tested.

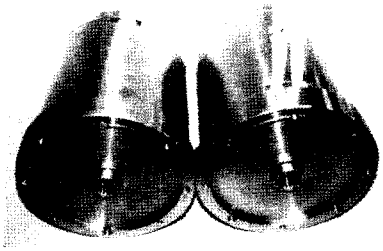

Fig. 6 Prototype 6/4 and 12/8 SRM

For the switching angle control, 2-channel, 10bit D/A converters and TMS320F241 DSP controllers are used. The calculated switching-on angle in the form of digital data is output to the first channel of the D/A converter as analog data, then the switching-off angle is output to the other channel of the D/A converter.

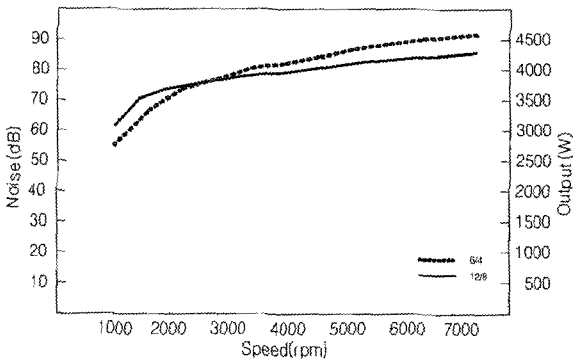

Fig. 7 Acoustic noise measurement of the prototype SRM

Fig 7 shows the measured acoustic noise comparison of the prototype SRM. As shown in Fig. 7, the experimental results show that higher acoustic noise occurs in the 6/4 SRM than in the 12/8 SRM.

Fig. 8 shows the measured efficiency of the prototype SRM according to speed and exciting angle. From the FEM analysis, the efficiency of the 6/4 SRM is higher than that of the 12/8 SRM.

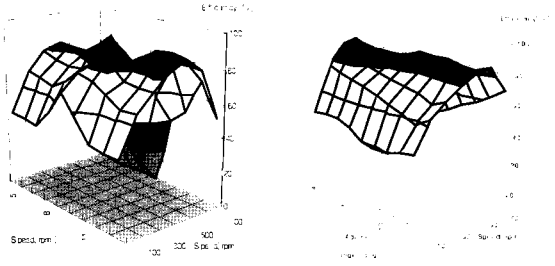

(a) 6/4 SRM (b)12/8 SRM

Fig. 8 Comparison of efficiency according to speed and exciting angle

4. The Multi-level Inverter

4.1 Excitation Control

For the proper application of an SRM to a LSEV, a high performance, stable inverter system is required. The classic inverter is very simple and effective but the control of the regenerative mode is not easy. The regeneration is essential in the EV application because of energy efficiency and dynamic braking during deceleration.

In this paper, a multi-level inverter topology is proposed to quickly magnetize and demagnetize during the motoring and regenerative mode with flat-topped current. Fig. 9 shows the proposed excitation voltage level in the motoring and regenerative mode. The high C-Dump voltage is used to quickly build-up current and to quickly extinguish current when switched off and also to quickly build-up generating current.

When an SRM is operated in single-pulse mode in regenerative mode, it is difficult to develop the rated output. A discontinuous PWM mode is used to improve regenerative power.

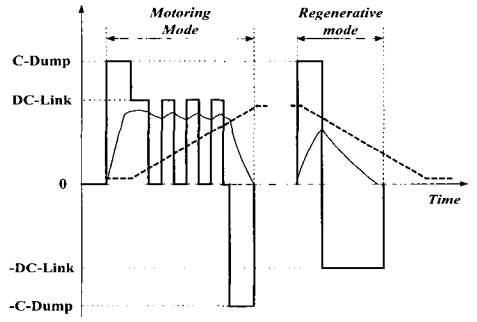

Fig. 9 5-level excitation voltage control

In order to satisfy these conditions, a circuit is proposed as shown in Fig. 10, which is able to generate a high voltage for building-up current and maintaining a source voltage for motoring and regenerative operating.

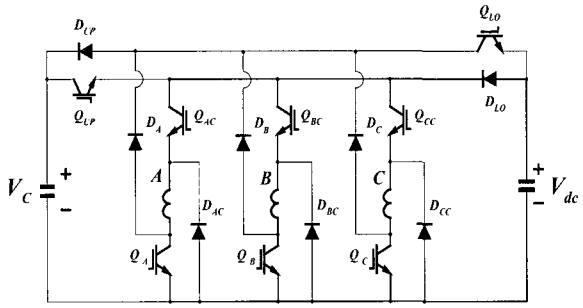

Fig. 10 The proposed 5-level inverter

The operations can be separated into four modes and the circuit of each mode is shown in Fig. 11.

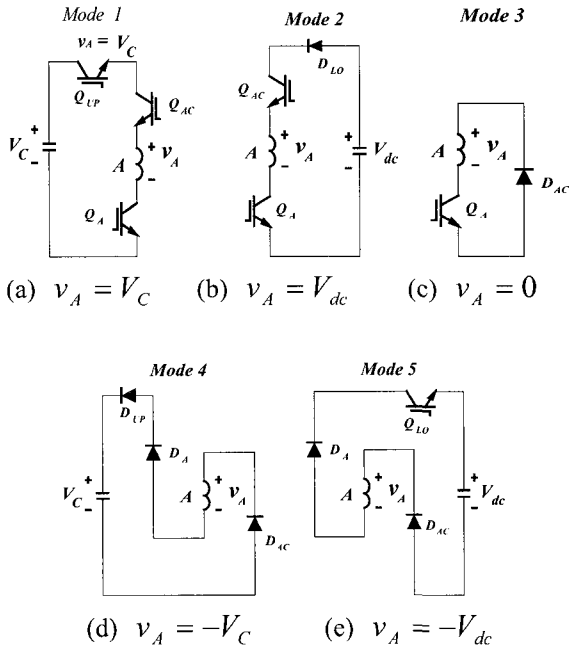

Fig. 11 Operation modes of the proposed 5-level inverter

(a) Mode 1 :

When Q_{UP}, Q_{AC}, Q_A is switched on, the capacitor voltage is impressed on phase winding. The high C-dump voltage, which is charged in the capacitor, is used to quickly build up phase current in motoring mode without excessive advanced angle for proper flat-topped current.

(b) Mode 2 :

When Q_{AC}, Q_A is switched on, the D.C. link voltage is impressed on phase winding. When the phase current is PWM controlled, the higher C-dump voltage is not good for smooth current control. This mode is proper for a current control method.

(c) Mode 3 :

When Q_A is switched on, a commutation circuit is created by diode D_A such that zero voltage is impressed on phase winding. This mode is proper for a current control method.

(d) Mode 4 :

When the switch is turned off completely, a circuit is created by diode D_{UP}, D_A, D_{AC} such that the opposite polarity of the capacitor voltage is impressed on phase winding. The high negative C-dump voltage quickly extinguishes the current when the motor is switched off.

(e) Mode 5 :

When Q_{LO} is switched on, the negative sign of the source voltage is impressed on phase winding. And the recovery energy is transferred to the side of the source.

The operation of this circuit is selected by switch Q_{LO} from the source and C-Dump voltage and in the regenerative region, though the regenerative lasts for a long time, the recovery energy is transferred to the source without the chopper. This operation is different from a conventional C-Dump circuit.

In the proposed control method, the fast response has the same characteristic as the delta modulation method. It can also operate at a constant switching frequency.

4.2 Switching Topology of the Multi-level Inverter

With the proposed multi-level inverter, an additional freewheeling mode is added to achieve a near unity energy conversion ratio which is very effective under light loads. The stored energy of a motor is not recovered to the source but transferred as mechanical power that is generated by phase current and back-emf. If the increasing period of inductance is sufficiently large compared with the additional mode, the stored field energy in inductance can be entirely converted into mechanical energy; then the energy conversion ratio approaches to unity.

Fig. 12 shows a graphical analysis of the field energy conversion process of the conventional method and the proposed switching method with a multi-level inverter.

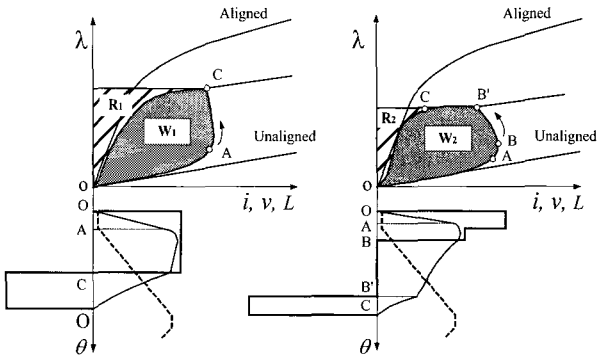

(a) conventional (b) proposed

Fig. 12 Energy conversion process

Under an unaligned position, during the current build-up period both methods show an equivalent path for energy conversion between O and A. But in other modes, because of an additional wheeling period, the proposed method forms path B'C resulting in a considerable increase to the energy conversion ratio. In the conventional method, the path follows AC. In path B'C, the stored energy in the field is transferred as a mechanical output. The total flux linkage maintains a near constant form, because the decrease of the current can be compensated for by the increase of the inductance. The path CO shows a demagnetizing mode. The proposed wheeling mode converts the field energy into mechanical energy without returning to the source. An additional wheeling mode can enlarge the field energy region converted to mechanical output; therefore, the reactive power will be decreased.

Fig. 13 shows the experimental waveform of phase current and flow through the energy recovery capacitor in the multi-level inverter.

It was tested in steady-state under the command speed 4000[rpm] at a rated load. From the experimental results, magnetizing, wheeling and demagnetizing periods appear at approximately 7°, 10°, 20° and 5°, respectively. As shown in the experimental results, to obtain a fast demagnetizing, high excitation voltage is applied, and the recovered capacitor voltage is used to settle current rapidly. Its displacement is proportional to the recovered energy.

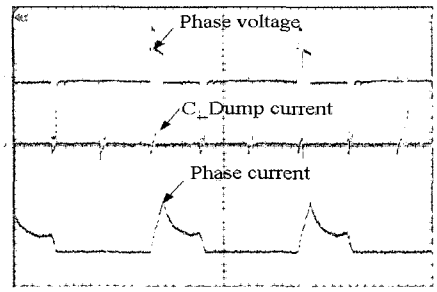

Fig. 13 Voltage and current waveforms of proposed inverter

Fig. 14 shows the capacitor voltage, phase voltage and current in regenerative mode.

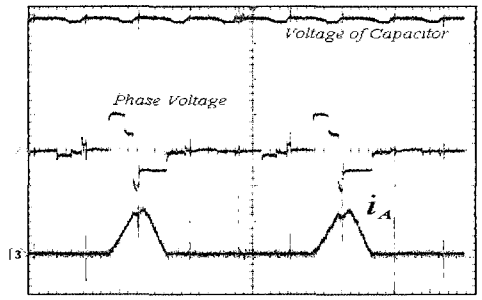

Fig. 14 Voltage and phase current in regenerative mode

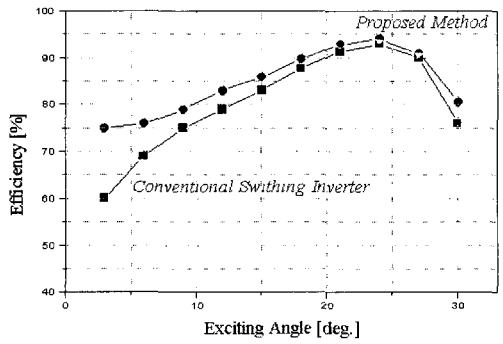

Fig. 15 Comparison of efficiency according to the switching method

Fig. 15 shows the efficiency comparison of the conventional and the proposed switching method in case of 6/4 SRM. When the excitation angle is small, considerable efficiency improvement is possible. The proposed wheeling mode is effective under a light load as shown in Fig. 15.

With the increase of the exciting angle, the proposed method has almost the same efficiency as that of the conventional method because the wheeling period is small.

5. An analog encoder for precise angle control

5.1 Conventional Encoder

In general, an optical encoder which has a digital pulse signal is often used in motor control systems because of its high performance, easy treatment of data and programming of controller. The information of rotor position and speed is obtained in a control period by the digitalized encoder such as an incremental or an optical encoder.

However, general optical encoders, such as incremental and absolute encoders are not suitable for SRM systems because of their cost and their inability to be used in harsh operating environments which include mechanical vibration and high speed. These days, high resolution serial absolute encoders are being considered for industrial applications. But, the cost is much higher and the maximum operating speed is generally limited to 8000[rpm].

For these reasons, a simple disk plate encoder with an optical sensor is used in the SRM system as shown in Fig. 16.

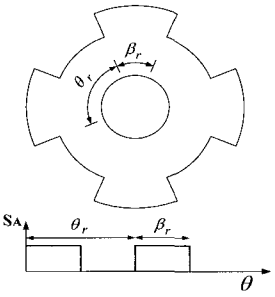

Fig. 16 A simple optical encoder disk and sensor signal

The structure of the optical encoder is very simple and inexpesive but the high resolution switching angle control is very difficult. The switching-on and off angle have to be calculated from all of the rising and falling edges of the optical encoder signals. The accuracy of the calculated switching angle depends on the microprocessor and rotor speeds. In this case, a simple PWM method is adopted for torque control. High frequency switching increases switching losses.

5.2 Proposed Analog Encoder

In order to maintain an accurate switching angle, a high resolution encoder and a proper control method are essential. This paper proposes a new type of encoder for switching angle control. The proposed encoder is simple but high resolution switching control is possible.

Fig. 17 shows the proposed analog encoder for 6/4 and 12/8 SRM's, respectively. The output signal of the proposed encoder is an analog signal which is proportional to a gray gradation of the plate. This is a digital signal in the conventional encoders such as incremental and optical encoders. The gray gradation of the disk plate is set for the linear analog signal of the photo transistor. The output of the photo-transistor is a triangular wave, which is the function of the position angle; therefore, the rotor position of the SRM can be obtained by the output voltage of the photo-transistor.

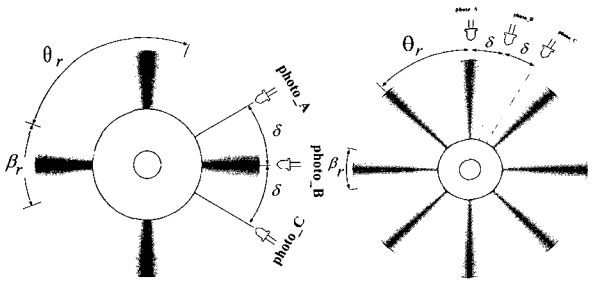

(a) 6/4 SRM (b) 12/8 SRM

Fig. 17 Disk plate of the proposed analog encoder

The interval between the gradated pattern is determined by the number of rotor poles N_r as follows.

$$\theta_r = \frac{2\pi}{N_r} \text{ [rad]} \tag{4}$$

And the minimum angle of a gradation is determined by the continuous torque production as follow.

$$\beta_r \geq 2\frac{2\pi}{N_s N_r} \text{ [rad]} \tag{5}$$

where, N_s and N_r denote the number of stator and rotor poles, respectively. In Fig. 17, the sensor interval δ denotes the phase intervals of the SRM. Therefore, δ is 15° in 8/6 and 12/8 and 30° in a 6/4 SRM.

Fig. 18 shows the output signal of the proposed encoder according to the inductance profile. The dip point θ_o of the output signal is the center point of the maximum dwell angle β_r of the proposed encoder. The advance angle θ_a and the delay angle θ_d are determined by the excitation voltage, rated current and motor parameters. In the motoring mode, the switching-on angle is set on the negative slope of the output signal between θ_a and θ_o. Similarly, a switching-off angle can be set on the positive slope of the output signal between θ_o and θ_d. The end of the negative and positive slopes of the encoder signal have a step shape for the limitation of the excitation interval in the maximum dwell angle β_r.

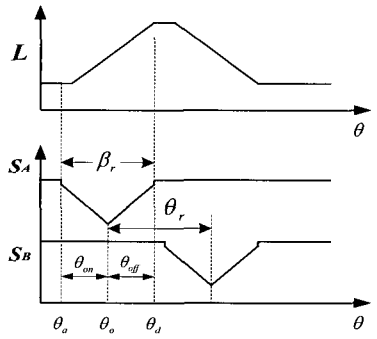

Fig. 18 Inductance profile and encoder signal

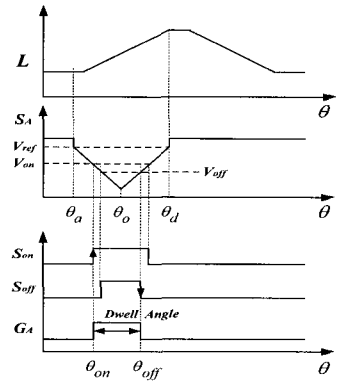

Fig. 19 Switching angle control of a phase

Using the proposed simple encoder, a very accurate switching angle control can be obtained without any high performance microprocessor.

5.3 Switching Angle Control Topology

Fig. 19 shows the principles of the switching angle

control topology with the proposed analog encoder. According to the motor speed and load condition, the proper switching-on angle θ_{on} and switching-off angle θ_{off} can be controlled independently by the command signals V_{on} and V_{off}, respectively. The advance angle θ_{on} is set at the cross point of the negative slope of the sensor signal, and the switching-on command signal V_{on} as follows.

$$\theta_{on} = \left(1 - \frac{V_{on}}{V_{ref}}\right)(\theta_o - \theta_a) + \theta_a \tag{6}$$

The maximum switching-on angle occurs in the minimum inductance region, so fast build-up of current is possible at the rated load. And the minimum switching-on angle occurs in the increasing region of inductance, so smooth build-up of current is possible at a light load with a smooth torque production.

Similarly, the delay angle θ_{off} is set at the cross point of the positive slope of the signal and the switching-off command signal V_{off}.

$$\theta_{off} = \frac{V_{off}}{V_{ref}}(\theta_d - \theta_o) + \theta_o \tag{7}$$

And the dwell angle is set to the interval between switching-on and off angle.

$$\theta_{dwell} = \theta_{off} - \theta_{on} \tag{8}$$

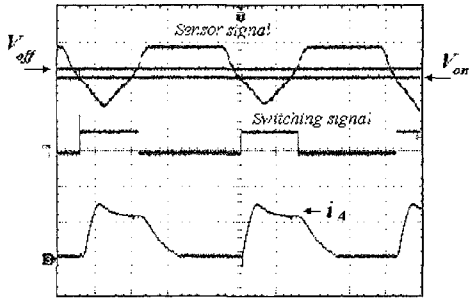

Fig. 20 Encoder, switching signal and phase current

Fig. 20 shows the sensor signal, switching-on reference, switching signal and phase current. The waveform of the phase current is determined by the sensor signal and switching command at 1750[rpm].

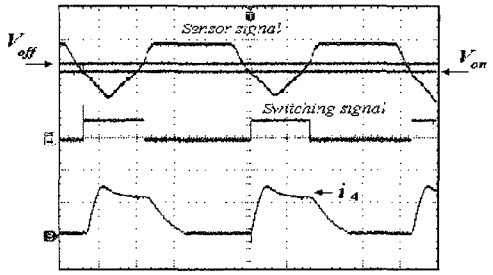

Fig. 20 Encoder, switching signal and phase current

Fig. 21 shows the switching angle adjustments and phase current according to load variations in the proposed encoder and control system at 2000[rpm]. The switching angle is increased by the changing of the switching-on reference. With a sudden load variation, the switching angle can be controlled properly, so a smooth torque production is possible. The experimental results show the effectiveness of the proposed encoder and control method.

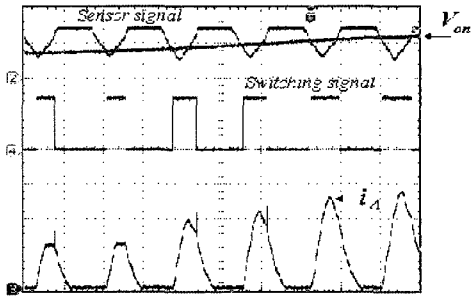

Fig. 21 Encoder signal and current with increasing of load

6. Conclusions

This SRM drive system for the LSEV application is designed with a new analog encoder and multi-level inverter. In the design process of the prototype SRM, the parameters are determined from CAD and FEM analysis results according to rotor and stator factors.

The motor is designed to be highly efficient and have low noise characteristics. Two types of prototype motors are designed and tested. A 12/8 motor is good for minimizing noise, while a 6/4 motor is good for power and efficiency.

For the switching angle control, a low cost, simple control method using a high performance analog encoder was proposed to maintain a practical and stable drive. The proposed encoder uses a simple optical encoder and

analog gradation for high resolution of the load position. The switching angle control can easily be implemented by using separated command signals for switching-on and switching-off.

In addition, a five-level inverter is used to build-up and extinguish phase current quickly. A high level of demagnetizing voltage is used to prevent a divergence of phase current during the regenerative mode. Also, current level control is unsuitable. The peak current controller is proposed to be able to improve the transient response and keep the switching frequency constant. The regenerated energy is used effectively because the motoring interval is minimized and the regenerative interval is increased relative to the motoring interval.

From the experimental results, the effectiveness of the proposed system with a proper control method is verified.

Acknowledgments

This work was supported by a Brain Busan 21 Project from Busan metropolitan city.

References

[1] R. B. Inderka, M. Menne, R. DeDoncker, "Control of Switched Reluctance Drive for Electric Vehicle Applications", IEEE Trans. Power Electronics, vol. 49, no. 1, pp. 48-53, 2002.

[2] P. J. Lawrenson, J.M. Stephenson and P. T. Blenkinsop et al, "Variable-speed Switched Reluctance Motors", IEE Proc. B, vol.127, no.4, 1980, pp.253-265.

[3] J. W. Ahn et al, "Novel Encoder for SRM Drive with High Resolution Angle Control", Proceedings of IEEE/ISIE 2001, pp. 1781-1785, 2001.

[4] J. W. Ahn et al, "High Energy Conversion Strategy of SRM with Single-pulse Switching", Proceedings of IEEE/ISIE 2002, pp. 695-700, 2002.

[5] C. Wu and C. Pollock, "Analysis and Reduction of Vibration and Acoustic Noise in the Switched Reluctance Drive", IEEE Trans. Industrial Applications, vol. 31, no. 1, pp. 91-98, 1995.

Jin-Woo Ahn was born in Busan, Korea, in 1958. He received the B.S., M.S., and Ph.D. degrees in Electrical Engineering from Pusan National University, Busan, Korea, in 1984, 1986, and 1992, respectively.

He has been with Kyungsung University, Busan, Korea, as a professor in the Department of Electrical and Mechanical Engineering since 1992. He was a Visiting Professor in the Dept. of EE, Glasgow University, U.K in 1995 and UW-Madison, USA in 1998. He is the author of several books and has several patents related to SR motors. He is also the author of more than 100 papers. His current research interests are motor drive systems and electric vehicle drives. He has been awarded several prizes including Best Paper in 2002, an academic achievement prize in 2003 from the Korean Institute of Electrical Engineers and an academic achievement prize in 2003 from the Korean Institute of Power Electronics, and the Best Paper prize in 2003 from The Korean Federation of Science and Technology Societies. He is an editorial director of KIEE Society of Electrical Machinery and Energy Conversion and an academic director of Korean Institute of Power Electronics. Dr. Ahn is a life-time member of the Korean Institute of Electrical Engineers, a member of the Korean Institute of Power Electronics and a senior member of IEEE.

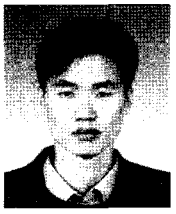

Dong-Hee Lee was born on Nov. 11, 1970 and received the B.S, M.E, and Ph. D. degrees in Electrical Engineering at Pusan National University, respectively. His major research field are motor drive systems and micro-process applications. He is a member of KIEE and currently works as a senior researcher at OTIS-LG.

Tae-Hyoung Kim was born on Dec. 11, 1977 and received the B.S in Electrical Engineering from Kyungsung Univ. His major research fields are motor drive systems and motor design. He is a member of KIEE and currently in graduate school at Kyungsung Univ.